

Iron–Sulfur Cluster Interconversions in Biotin Synthase: Dissociation and Reassociation of Iron during Conversion of [2Fe-2S] to [4Fe-4S] Clusters[†]

Natalia B. Ugulava, Brian R. Gibney, and Joseph T. Jarrett*

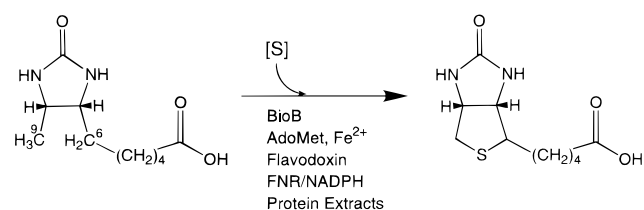
Johnson Research Foundation and Department of Biochemistry and Biophysics, University of Pennsylvania, Philadelphia, Pennsylvania 19104

Received November 12, 1999; Revised Manuscript Received February 16, 2000

ABSTRACT: Biotin synthase catalyzes the insertion of a sulfur atom into the saturated C6 and C9 carbons of dethiobiotin. This reaction has long been presumed to occur through radical chemistry, and recent experimental results suggest that biotin synthase belongs to a family of enzymes that contain an iron–sulfur cluster and reductively cleave *S*-adenosylmethionine, forming an enzyme or substrate radical, 5′-deoxyadenosine, and methionine. Biotin synthase (BioB) is aerobically purified as a dimer of 38 kDa monomers that contains two [2Fe-2S]²⁺ clusters per dimer. Maximal *in vitro* biotin synthesis requires incubation of BioB with dethiobiotin, AdoMet, reductants, exogenous iron, and crude bacterial protein extracts. It has previously been shown that reduction of BioB with dithionite in 60% ethylene glycol produces one [4Fe-4S]^{2+/1+} cluster per dimer. In the present work, we use UV/visible and electron paramagnetic resonance spectroscopy to show that [2Fe-2S] to [4Fe-4S] cluster conversion occurs through rapid dissociation of iron from the protein followed by rate-limiting reassociation. While in 60% ethylene glycol the product of dithionite reduction is one [4Fe-4S]²⁺ cluster per dimer, the product in water is one [4Fe-4S]¹⁺ cluster per dimer. Further, incubation with excess iron, sulfide, and dithiothreitol produces protein that contains two [4Fe-4S]²⁺ clusters per dimer; subsequent reduction with dithionite produces two [4Fe-4S]¹⁺ clusters per BioB dimer. BioB that contains two [4Fe-4S]^{2+/1+} clusters per dimer is rapidly and reversibly reduced and oxidized, suggesting that this is the redox-active form of the iron–sulfur cluster in the anaerobic enzyme.

The final step in the biosynthesis of biotin is the insertion of a sulfur atom between the C6 and C9 carbons of dethiobiotin (Scheme 1), a reaction catalyzed by biotin synthase. The *bioB* gene product has been identified as an essential component of biotin synthase by genetic complementation (1, 2), and addition of overexpressed BioB protein to *in vitro* assays increases biotin yield (3, 4). BioB is a dimer of 38.5 kDa monomers that is purified under aerobic conditions with two [2Fe-2S]²⁺ clusters per BioB dimer (5). The predicted protein sequence contains a conserved Cxxx-CxxC motif that is shared by pyruvate formate-lyase activating enzyme (PFL AE) (6), type III (anaerobic) ribonucleotide reductase (anRR) (7), lysine 2,3-aminomutase (8), and lipoic acid synthase (LipA) (9). PFL AE and anRR have been shown to use AdoMet and reduced flavodoxin to catalyze formation of an essential glycy radical on the protein backbone (10–13), while lysine 2,3-aminomutase appears to use AdoMet to catalyze direct formation of substrate radical (14, 15). BioB-catalyzed biotin formation is increased by the addition of AdoMet and flavodoxin (3, 4, 16–18), and therefore it has been proposed that BioB is

Scheme 1: Conversion of Dethiobiotin to Biotin Catalyzed by Biotin Synthase



also an AdoMet-dependent radical enzyme (16).

Radical enzymes play critical roles in biology (19), and enzymatic radical generation must take place under both aerobic and anaerobic conditions. One solution to enzymatic radical generation in the absence of oxygen is the reductant-induced oxidation of enzyme or substrate using AdoMet and an iron–sulfur cluster (20). In a generalized scenario, AdoMet binds near the iron–sulfur cluster and electron transfer from flavodoxin into the iron–sulfur cluster/AdoMet complex results in reductive cleavage of AdoMet, generating

[†] This research has been supported by NIH Research Grant GM59175 (J.T.J.), the Thomas B. and Jeannette E. Laws McCabe Fund, and the University of Pennsylvania Research Foundation.

* Correspondence should be addressed to this author at the Department of Biochemistry and Biophysics, University of Pennsylvania School of Medicine, 905B Stellar-Chance Laboratories, Philadelphia, PA 19104-6059. E-mail: jjarrett@mail.med.upenn.edu; fax 215-573-8052.

¹ Abbreviations: AdoHcy, *S*-adenosyl-L-homocysteine; AdoMet, *S*-adenosyl-L-methionine; anRR, anaerobic (type III) ribonucleotide reductase; DTT, dithiothreitol; EDTA, ethylenediaminetetraacetic acid; EPR, electron paramagnetic resonance; Fld, flavodoxin; FNR, ferredoxin (flavodoxin); nicotinamide adenine dinucleotide phosphate oxidoreductase; NADPH, nicotinamide adenine dinucleotide phosphate, reduced form; NADP⁺, nicotinamide adenine dinucleotide phosphate; PFL AE, pyruvate formate-lyase activating enzyme; Tris, tris(hydroxymethyl)aminomethane hydrochloride.

methionine and the strongly oxidizing 5'-deoxyadenosyl radical (21). Abstraction of a hydrogen atom either from a glycyl residue or from the substrate results in oxidation to a glycyl radical (22–24) or substrate radical (14) and formation of 5'-deoxyadenosine (25). The structures and redox states of iron–sulfur clusters in the active enzymes and the mechanism of the reductive cleavage of AdoMet remain a mystery.

Recent spectroscopic studies have established the flexibility of the conserved iron–sulfur cluster-binding motif in PFL AE, anRR, lysine 2,3-aminomutase, LipA, and BioB. PFL AE is overexpressed and purified under anaerobic conditions containing predominantly [3Fe-4S]¹⁺ clusters that are easily converted to the [4Fe-4S]²⁺ and [4Fe-4S]¹⁺ clusters upon reduction with dithionite in the absence and presence of AdoMet (26). Overexpressed and reconstituted anRR contains two [2Fe-2S]²⁺ clusters per $\alpha_2\beta_2$ tetramer that are converted to one [4Fe-4S]^{2+/1+} cluster upon reduction with dithionite or 5-deazaflavin/formate, as demonstrated by EPR and Mossbauer spectroscopy (27). Lysine 2,3-aminomutase is purified anaerobically, containing six [4Fe-4S]²⁺ clusters per hexamer that are converted to [4Fe-4S]¹⁺ clusters upon reduction with dithionite in the presence of AdoMet or AdoHcy (28). Overexpressed LipA is purified under anaerobic conditions as a mixture of monomer that contains one [2Fe-2S]²⁺ cluster and dimer that contains one [4Fe-4S]²⁺ cluster (29, 30). Finally, BioB purified aerobically contains two [2Fe-2S]²⁺ clusters per dimer that are converted to one [4Fe-4S]²⁺ cluster upon reduction with dithionite in 60% ethylene glycol (31). The observation of several iron–sulfur cluster configurations within the same conserved binding motif suggests that these proteins share the ability to retain bound iron and sulfide under conditions of both high and low redox potential; this may confer an evolutionary advantage for facultative anaerobes that must tolerate exposure to high oxygen levels. In the case of lysine 2,3-aminomutase, the [4Fe-4S]^{1+/AdoMet} form of the enzyme is active in the absence of exogenous reductant, suggesting that the [4Fe-4S]^{1+/AdoMet} to [4Fe-4S]^{2+/5'-deoxyadenosine} conversion may represent the native cluster conversion (28).

Reductive conversion of BioB from the aerobically purified [2Fe-2S]²⁺ forms requires experimental conditions that bring into question the likelihood of a similar *in vivo* cluster conversion. Johnson and co-workers (31) report that incubation of BioB in 60% ethylene glycol or glycerol with the strong reductant sodium dithionite produces [4Fe-4S]²⁺ protein over 4–5 h. [4Fe-4S]¹⁺ cluster formation is only observed at moderate levels following prolonged incubation with a large excess of dithionite. The slow kinetics of this process suggests that it is unlikely to occur in rapidly growing bacteria that must have active biotin synthase to form biotin within the ca. 30–60 min doubling time of the organism. The apparent *in vivo* reducing system, flavodoxin, FNR, and NADPH, does not bring about cluster conversion in water or 60% ethylene glycol (J. Jarrett, unpublished results).

We have used UV/visible and EPR spectroscopy to examine the kinetics of [2Fe-2S]²⁺ to [4Fe-4S]^{2+/1+} cluster conversion in 60% ethylene glycol, conditions similar to those used by Duin et al. (31), as well as in aqueous buffer. We find that under all conditions, cluster conversion is a two-step process in which iron is rapidly released from the protein and then slowly reabsorbed. Reduction of BioB with

dithionite in the presence of iron chelators terminates cluster conversion and results in precipitation of apoprotein. Reduction in the presence of excess iron and/or sulfide results in an increase in the rate of cluster conversion and an increase in the yield of [4Fe-4S]^{2+/1+} clusters. While in the absence of excess iron the principal product of reduction is one [4Fe-4S]^{2+/1+} cluster per BioB dimer, the product in the presence of excess iron and sulfide is two [4Fe-4S]^{2+/1+} clusters per BioB dimer. BioB containing two [4Fe-4S]^{2+/1+} clusters per dimer undergoes rapid and reversible chemical reduction and oxidation. Although our present assay system is not able to distinguish the active forms of BioB, we believe that this latter redox interconversion is comparable to the presumed flavodoxin-dependent reduction of the iron–sulfur clusters in the native enzyme.

MATERIALS AND METHODS

Materials. All reagents were obtained from commercial sources and used without further purification. Protein concentration was determined by the Bradford assay (32) with bovine serum albumin as a standard, or for BioB in the [2Fe-2S]²⁺ oxidation state, with a molar absorption for the dimer of $\epsilon_{452} = 7550 \text{ M}^{-1} \text{ cm}^{-1}$. The UV/visible spectrum and the Fe/protein ratio is very reproducible between preparations, and therefore we feel that the visible absorbance is a reliable method for determining the concentration of the freshly purified [2Fe-2S]²⁺ protein. Iron analysis was performed by the method of Beinert (33); sulfide analysis was not performed. Free iron was separated from protein-bound iron by passing through a short desalting column (for protein iron analysis, PD-10, Amersham Pharmacia) or by passing through a 30 kDa cutoff centrifugal concentrator (for free iron, Millipore). Unless otherwise stated, all protein purification steps were performed under aerobic conditions and all protein reduction, reconstitution, and analyses were performed under oxygen-free argon or nitrogen atmosphere.

Cloning and Expression of BioB and His-Tagged BioB. BioB was cloned by direct PCR from a lysate of Kohara phage [202]3D4 (34) using VENT polymerase and primers that contained *NdeI* and *HindIII* sites. The PCR product and pET23b (Novagen) were digested with *NdeI* and *HindIII* and joined with T4 DNA ligase. The resulting vector (pJJ07) was transformed into BL21(DE3)pLysS. In a typical preparation of BioB protein, 1 L of LB containing 10 μM FeCl₃, 50 mg/L ampicillin, and 25 mg/L chloramphenicol was inoculated with 5 mL of an overnight culture of pJJ07/BL21(DE3)pLysS in the same medium. The culture was incubated at 37 °C with vigorous shaking for 4–5 h and then induced with 0.5 mM IPTG. Protein expression was continued for 4 h and the cells were collected by centrifugation and frozen at –80 °C. The cells were suspended in 50 mM Tris, pH 7.5, and lysed by sonication, and cell debris was removed by centrifugation at 25 000 rpm for 30 min. The protein was loaded onto DEAE fast-flow Sepharose (2.5 × 20 cm, Sigma) equilibrated with 50 mM Tris, pH 7.5, and eluted with a 300 mL linear gradient to 0.6 M NaCl, 50 mM Tris, pH 7.5. Reddish-brown fractions were collected, concentrated, and desalted with Centriprep 30 concentrators (Millipore). The desalted protein was loaded onto a Poros HQ column (10 × 100 mm, PE/PerSeptive Biosystems) equilibrated in 50 mM Tris, pH 8, and eluted with a 150 mL linear gradient to 0.6 M NaCl, 50 mM Tris, pH 8. The

protein was concentrated and desalted with Centriprep 30 concentrators. The resulting protein varies from 70% to 90% homogeneous. Further purification invariably resulted in a dramatic loss of activity.

BioB was subcloned into a His tag expression plasmid constructed by Professor Greg Van Duyne (University of Pennsylvania). This plasmid (pET21dHT) is derived from pET21d (Novagen), in which the BioB protein is fused to a 6×His tag by an extended linker peptide that contains a TEV protease site. BioB was cloned from pJJ07 by use of primers that incorporated *Bam*HI and *Eco*RI restriction sites. The PCR product and pET21dHT were digested with *Bam*HI and *Eco*RI and joined with T4 DNA ligase. The resulting vector (pJJ15-4A) was transformed in BL21(DE3)pLysS. In a typical preparation of His₆-BioB protein, 1 L of LB with 10 μM FeCl₃, 50 mg/L ampicillin, and 25 mg/L chloramphenicol was inoculated with 5 mL of an overnight culture of pJJ15-4A/BL21(DE3)pLysS in the same medium. The culture was incubated at 37 °C with vigorous shaking for 5 h, cooled to 25 °C, and then induced with 0.5 mM IPTG. Protein expression was continued for 4 h at 25 °C, and the cells were collected by centrifugation and frozen at -80 °C. The cells were suspended in 50 mM Tris, 0.5 M NaCl, pH 8, and lysed by sonication, and cell debris was removed by centrifugation at 25 000 rpm for 30 min. The protein was loaded onto Ni-NTA-agarose (2.5 × 10 cm, Qiagen) and washed with 300 mL of 50 mM Tris, 0.5 M NaCl, pH 8, and 200 mL of 10 mM imidazole in the same buffer. His₆-BioB is eluted with 200 mM imidazole, 50 mM Tris, 0.5 M NaCl, pH 8, and concentrated with Centriprep 30 concentrators to ~10 mL. To remove imidazole, the protein is immediately loaded onto a Bio-Gel P2 column (2.5 × 40 cm, Bio-Rad) equilibrated with 25 mM Tris, 25 mM NaCl, pH 7.5, and the protein was eluted in the same buffer. The resulting 41.3 kDa protein is >98% homogeneous as judged by SDS-polyacrylamide gel electrophoresis. Attempts at removal of the His₆ tag with TEV protease lead to proteolytic cleavage of a 4–6 kDa fragment from the C-terminus of protein, yielding a 32–34 kDa protein that retained the bound FeS cluster; we have avoided using this protein since it is unclear what role this missing C-terminal fragment may play in the protein structure.

Due to the abundant yield of His₆-BioB and the relatively high purity as compared to native (non-His-tagged) BioB, we have used His₆-BioB in all of the experiments described in this paper. We have repeated both UV/visible and EPR experiments with native BioB and obtained the same results within the errors of our measurements. However, the quality of the EPR spectra is significantly improved for His₆-BioB, and we therefore present only the data for this modified protein. Using EPR spectroscopy, we could not detect significant amounts of iron bound to the His₆ tag in either as-purified [2Fe-2S]²⁺ protein or reconstituted [4Fe-4S]^{2+/1+} protein.

Reduction of BioB with Sodium Dithionite. All experiments were performed under anaerobic conditions either in a glovebox under nitrogen atmosphere or in sealed Schlenk tubes or cuvettes under an argon atmosphere. BioB or His₆-BioB was diluted into 25 mM Tris, 25 mM NaCl, pH 7.5, with or without 60% (v/v) ethylene glycol, and the protein solution (50–500 μM, 1 mL) was placed in an anaerobic cuvette and capped with a tightly sealed rubber septum. The

sample was purged with cycles of vacuum and argon over 30 min to remove oxygen. A UV/visible spectrum of the BioB protein was recorded and dithionite (2–4 mM final concentration) was added with a syringe to initiate reduction. UV/visible spectra were recorded at intervals over several hours, and at various stages of reduction a sample (~200 μL) was removed for EPR analysis.

Reduction in the Presence of Excess Iron and Sulfide. BioB or His₆-BioB was diluted into 10 mM dithiothreitol, 25 mM Tris, 25 mM NaCl, pH 7.5, with or without 60% ethylene glycol, and the protein solution (100–200 μM, 1 mL) was placed in an anaerobic cuvette and purged with argon. Anaerobic solutions of FeCl₃ and Na₂S were slowly titrated into the protein solution to final concentrations of 0.5–1 mM. Precipitate was not observed and the protein spectrum is altered dramatically by these additions, resulting in a greenish-yellow sample. Excess iron, sulfide, and dithiothreitol were removed by passing through a desalting column equilibrated with 25 mM Tris and 25 mM NaCl, pH 7.5, in a nitrogen glovebox. The [4Fe-4S]¹⁺ protein was produced by addition of dithionite (2 mM), which resulted in immediate reduction of the protein within the time required to mix the contents of the cuvette accompanied by bleaching of the visible absorption band at 410 nm.

EPR Spectroscopy. Electron paramagnetic resonance (EPR) spectroscopy was performed on a Bruker ESP300E spectrometer operating at X-band frequencies. Temperature control was maintained by an Oxford ESR 900 continuous flow liquid helium cryostat interfaced with an Oxford ITC4 temperature controller. Microwave frequency was measured by a Hewlett-Packard 5350B frequency counter. Typical EPR parameters were as follows: sample temperature, 20 K; microwave frequency, 9.424 GHz; microwave power, 20 mW; modulation frequency, 100 kHz; modulation amplitude, 6.0 G; time constant, 164 ms. These conditions were shown to produce clean spectra without saturation of the EPR signals. Power saturation experiments were performed at 20 K with microwave powers between 50 μW and 200 mW. The temperature dependence of the [4Fe-4S]¹⁺ resonances were measured at 20 mW between 6 and 50 K. A 20 G modulation amplitude was employed to increase the iron-sulfur cluster signal during the power saturation and temperature dependence experiments. The concentration of unpaired spins was determined from a calibration curve based on Cu(II)-EDTA standards. Unless otherwise noted, total protein concentrations were 100–200 μM dimer.

Rate of [4Fe-4S] Oxidation/Reduction Measured by Stopped-Flow Spectroscopy. Stopped-flow spectroscopy was performed on a Hi-Tech DX-2 stopped-flow spectrophotometer that had been flushed with 10 mM dithionite for 24 h prior to use. Anaerobic samples of BioB in [4Fe-4S]²⁺ and [4Fe-4S]¹⁺ oxidation states were prepared in the presence of excess iron and sulfide and desalted into 25 mM Tris and 25 mM KCl, pH 7.5, as described above. The [4Fe-4S]²⁺ protein (50–100 μM final concentration) was rapidly mixed with dithionite (1 mM) at 25 °C, and absorbance changes were monitored at 410 nm. The [4Fe-4S]¹⁺ protein (50–100 μM) was rapidly mixed with K₃Fe(CN)₆ (500 μM) at 25 °C, and absorbance changes were monitored at 410 and 450 nm. Spectra were recorded prior to and following each kinetic run to determine the products of oxidation or reduction.

RESULTS

Formation of One [4Fe-4S]²⁺ Cluster per BioB Dimer Involves Dissociation and Reassociation of Iron. Generation of a protein or substrate radical in AdoMet-dependent radical enzymes requires the low-potential reductive cleavage of AdoMet, a process that is probably initiated by electron transfer from flavodoxin in *Escherichia coli* but can be achieved with dithionite in vitro. Although the mechanism of reductive cleavage has not been elucidated, it has been proposed that the reaction requires a special interaction between AdoMet and the conserved iron–sulfur cluster. In lysine 2,3-aminomutase, the apparent active form of the cluster is [4Fe-4S]¹⁺ (28), and it has now been demonstrated that all of the AdoMet-dependent radical enzymes are capable of forming a [4Fe-4S]^{2+/1+} cluster (26, 27, 29–31, 35, 36); it follows that activation of biotin synthase may require conversion of [2Fe-2S]²⁺ BioB to a [4Fe-4S]^{2+/1+} protein. Johnson and co-workers (31) demonstrated that reduction of BioB with dithionite in 60% ethylene glycol or glycerol results in the slow conversion of two [2Fe-2S]²⁺ clusters per dimer to one [4Fe-4S]²⁺ cluster per dimer.

We have followed cluster conversion in BioB after reduction with dithionite in 60% ethylene glycol using UV/visible and EPR spectroscopy (Figures 1–3). We find using UV/visible spectroscopy (Figure 1A and 2A) that the initial reduction of [2Fe-2S]²⁺ protein with dithionite occurs at a moderate rate ($k_{\text{obs}} = 0.2\text{--}1\text{ min}^{-1}$), while the formation of [4Fe-4S]²⁺ protein occurs much more slowly ($k_{\text{obs}} \approx 0.002\text{--}0.05\text{ min}^{-1}$). The range of rates reflects our inability to establish the total change in absorbance associated with each kinetic phase; we can fit the data reasonably well to models in which half or all of the iron is dissociated in the intermediate stage. Further, we have assumed that dissociated iron does not contribute to the UV/visible spectrum at 410 nm, but if iron and sulfide dissociate as a cluster, this may contribute to the observed absorbance of the intermediate. The overall reduction is accompanied by a shift in the visible absorption band at 452 nm for the [2Fe-2S]²⁺ protein to a shoulder centered at 410 nm for the [4Fe-4S]²⁺ protein (Figure 1A). The final yield of [4Fe-4S]²⁺ cluster is dependent on the initial concentration of protein and is ca. 60–70% after 4 h for an initial BioB concentration of 200 μM , assuming a typical extinction coefficient for the [4Fe-4S]²⁺ cluster of $\sim 7500\text{ M}^{-1}\text{ cm}^{-1}$ (37). The resulting biphasic kinetic curve suggests a maximal buildup at $\sim 10\text{--}30\text{ min}$ of intermediates that have little visible absorbance (Figures 1A and 2).

Two opposing interpretations of the above results are that the observed intermediate is either apoprotein and dissociated Fe²⁺ or BioB with two [2Fe-2S]¹⁺ clusters per dimer; [2Fe-2S]¹⁺ protein would be predicted to have little UV/visible absorbance but display a characteristic anisotropic EPR spectrum with $g_{\text{av}} \approx 1.9\text{--}2.0$ with maximal signal intensity observed at temperatures $\geq 50\text{ K}$ (37). However, EPR spectra of samples removed at 10, 30, and 90 min after reduction show only minor amounts of [4Fe-4S]¹⁺ cluster (less than 10% of total protein; Figure 3D,E) and also show variable amounts of dissociated iron ($g \approx 3.7\text{--}4.3$, not shown). Free iron is difficult to quantitate by EPR in dithionite-reduced samples and is difficult to chemically analyze in the presence of ethylene glycol; chemical measurements of free iron are

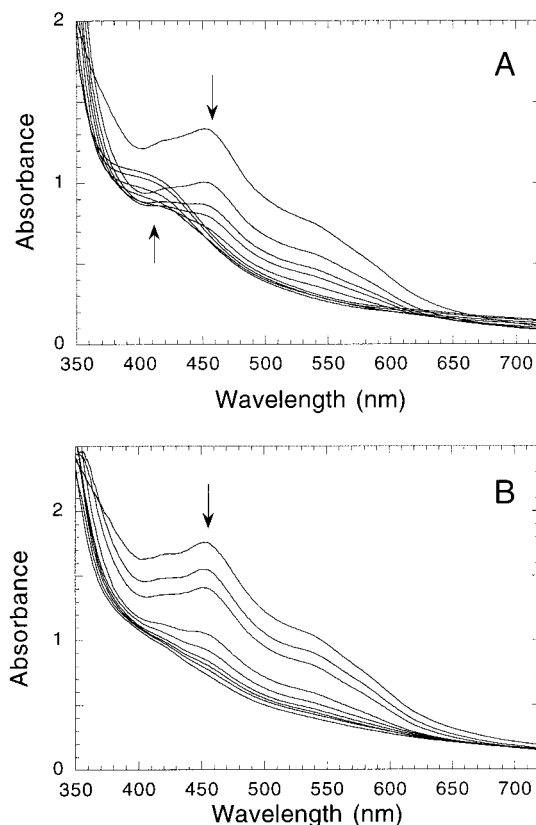


FIGURE 1: Reduction of [2Fe-2S]²⁺ BioB with dithionite. (A) Incubation of BioB (200 μM) with dithionite (2 mM) in 60% ethylene glycol, 25 mM Tris, 25 mM KCl, pH 7.5. Reduction of [2Fe-2S]²⁺ clusters results in a decrease in absorbance at 452 nm and probable formation of apoprotein. Slower reassociation of iron results in formation of a [4Fe-4S]²⁺ cluster as indicated by an increase in absorbance at 410 nm. (B) Incubation of BioB (200 μM) with dithionite (2 mM) in 25 mM Tris, 25 mM KCl, pH 7.5. Reduction of [2Fe-2S]²⁺ clusters results in a decrease in absorbance at 452 nm and the formation of protein with a featureless UV/visible spectrum that is shown by EPR spectroscopy to contain ~ 0.6 [4Fe-4S]¹⁺ clusters per dimer.

described below for samples reduced in water. The EPR spectrum of fully reduced enzyme after 4 h of incubation with dithionite shows formation of $\sim 0.1\text{--}0.2$ [4Fe-4S]¹⁺ cluster per dimer. The temperature dependence of the EPR signal for 10 min reduced and fully reduced samples shows a maximum intensity at $T = 20\text{ K}$, consistent with a [4Fe-4S]¹⁺ cluster (data not shown). The EPR spectrum for fully reduced [4Fe-4S]¹⁺ enzyme is similar to that observed by Johnson and co-workers (31), with g values of 2.04 and 1.93. Thus EPR spectra suggest that the [2Fe-2S]¹⁺ cluster is not a significant intermediate during reduction and that the final reduced protein is a mixture of [4Fe-4S]²⁺ and [4Fe-4S]¹⁺ protein, as previously observed.

[4Fe-4S] Cluster Formation Depends on the Availability of Free Iron. The conversion of apoprotein to [4Fe-4S]²⁺ protein requires the association of iron or of preformed iron–sulfur complexes with the apoprotein. We would predict, therefore, that the rate of formation of [4Fe-4S]²⁺ protein should be a second-order kinetic process dependent both on the concentration of free iron and on the concentration of apoprotein. Indeed we observe that when 200 μM BioB is reduced with dithionite in the presence of 500 μM FeCl₂, the rate of formation of [4Fe-4S]²⁺ protein (the second kinetic phase in Figure 2A) is increased ca. 4-fold ($k_{\text{obs}} = 0.02\text{--}$

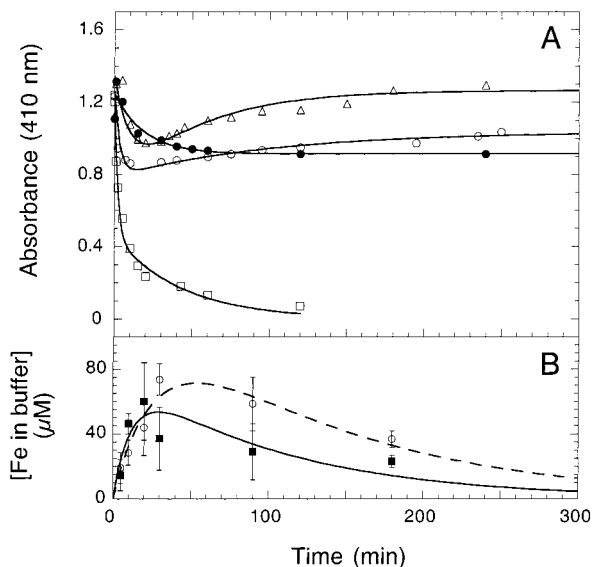


FIGURE 2: Kinetics of reduction of BioB (200 μM) with dithionite (2 mM) followed at 410 nm. (A) Reduction in 60% ethylene glycol (○) results in dissociation of iron accompanied by a decrease in absorbance ($k_{\text{obs}} \approx 0.2\text{--}1\text{ min}^{-1}$) and the slower formation of [4Fe-4S] $^{2+}$ protein with the appearance of a shoulder at 410 nm ($k_{\text{obs}} \approx 0.002\text{--}0.05\text{ min}^{-1}$). Reduction in the presence of FeCl_2 in 60% ethylene glycol (500 μM , Δ) results in an increase in the rate of [4Fe-4S] $^{2+}$ cluster formation with an increase in the rate constant for the second phase to 0.01–0.05 min^{-1} . Reduction in the presence of EDTA (2 mM, \square) in 60% ethylene glycol results in the complete formation of apoprotein with no absorbance remaining after 15 min. Reduction in aqueous buffer (●) results in a decrease in absorbance ($k_{\text{obs}} = 0.05\text{ min}^{-1}$) that reaches a plateau at $A_{410} = 0.9$, indicating the formation of a reduced protein-bound cluster. (B) Free iron found in the buffer following reduction of His $_6$ -BioB (■) or WT BioB (○) with dithionite in aqueous buffer. Conditions were identical to closed circles in panel A. Error bars indicate the standard deviation of three trials.

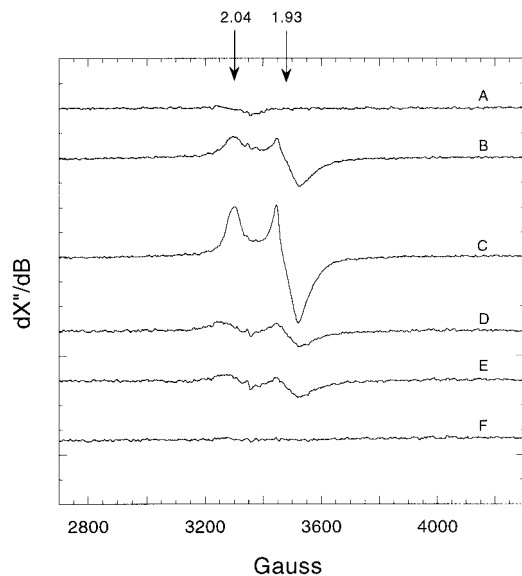


FIGURE 3: EPR spectra of intermediate and final stages of the reduction of BioB (200 μM) with dithionite (2 mM). (A) Initial [2Fe-2S] $^{2+}$ protein; (B) reduced 10 min with dithionite in aqueous buffer; (C) reduced 90 min with dithionite in aqueous buffer; (D) reduced 10 min with dithionite in 60% ethylene glycol; (E) reduced 90 min with dithionite in 60% ethylene glycol; (F) reduced 60 min with dithionite in EDTA (2 mM).

0.06 min^{-1}). Further, when the initial BioB concentration is increased to 500 μM in the absence of exogenous iron, the

rate of formation of [4Fe-4S] $^{2+}$ protein is increased ~ 2 -fold (not shown). Increasing the iron or protein also increases the final yield of [4Fe-4S] $^{2+}$ cluster to ~ 0.9 cluster per dimer based upon UV/visible spectra. This suggests that both the equilibrium concentration and the second-order rate of formation of the [4Fe-4S] $^{2+}$ cluster depends on iron and protein concentrations. In contrast to these results, when iron is competitively bound by chelation to either EDTA (2 mM) or L-histidine (5 mM) during reduction, we observe rapid loss of the [2Fe-2S] $^{2+}$ cluster ($k_{\text{obs}} = 0.5\text{ min}^{-1}$) as indicated by the disappearance of the absorbance band at 452 nm (Figure 2A), but the formation of both [4Fe-4S] $^{2+}$ and [4Fe-4S] $^{1+}$ clusters is completely blocked (see Figure 3F). The resulting sample is colorless, and white apoprotein precipitates over 30–60 min. The initial [2Fe-2S] $^{2+}$ protein is completely stable to EDTA for days, while the [4Fe-4S] $^{2+}$ protein (after removal of dithionite) loses iron very slowly in EDTA ($t_{1/2} \approx 12\text{--}15\text{ h}$). Together these results are consistent with a model in which formation of a [4Fe-4S] $^{2+}$ cluster in BioB is a second-order kinetic process involving association between apoprotein and iron or preformed iron-sulfur clusters.

Reduction of [2Fe-2S] $^{2+}$ BioB in the Absence of Ethylene Glycol Results in Formation of One [4Fe-4S] $^{1+}$ Cluster per Dimer. Due to the reported requirement for 60% ethylene glycol for assembly of the [4Fe-4S] $^{2+}$ cluster in BioB, and the slow time scale we had observed for this cluster conversion, we felt that it was unlikely that this process could precede AdoMet-dependent enzyme activation in either in vitro assays or in vivo biotin biosynthesis, both of which proceed in <30 min in the absence of ethylene glycol. Flint and co-workers (5) had reported the destruction of the iron-sulfur cluster upon treatment of [2Fe-2S] $^{2+}$ BioB with dithionite in aqueous buffer. We followed reduction of [2Fe-2S] $^{2+}$ BioB with dithionite using UV/visible and EPR spectroscopy and observed stoichiometric conversion to BioB containing ~ 0.6 [4Fe-4S] $^{1+}$ cluster per BioB dimer (Figures 1B and 3C). The UV/visible spectrum of the resulting [4Fe-4S] $^{1+}$ protein shows no distinct features but rather shows gradually increasing absorbance over the range from 300 to 600 nm (Figure 1B). Reduction occurs at approximately the same rate as in the presence of ethylene glycol, with an apparent rate constant of 0.05 min^{-1} (Figure 2, ●). EPR spectra of samples removed at 10, 30, and 90 min show formation of the [4Fe-4S] $^{1+}$ cluster with ~ 0.1 , 0.5, and 0.6 spin per dimer, respectively. The temperature dependence of the EPR signal for the 10 and 90 min samples (Figure 4) is characteristic of [4Fe-4S] $^{1+}$ clusters, with maximal signal observed at 20 K. The observed decrease in signal intensity and broadening of the resonance at lower temperatures is due to saturation of the signal. There is no EPR evidence for a stable [2Fe-2S] $^{1+}$ cluster in the early stages of reduction. Following complete reduction with dithionite in aqueous buffer, the EPR spectrum has an axial signal with g values of 2.04 and 1.93, identical to the spectrum obtained in the presence of ethylene glycol (Figure 3 and ref 31), but the yield is dramatically improved, with $>90\%$ of the protein-bound iron present in [4Fe-4S] $^{1+}$ clusters and $\sim 60\%$ of the total protein containing [4Fe-4S] $^{1+}$ clusters.

Since EPR spectroscopy had ruled out formation of stable [2Fe-2S] $^{1+}$ clusters immediately following dithionite reduction, the observed initial decrease in UV/visible absorbance

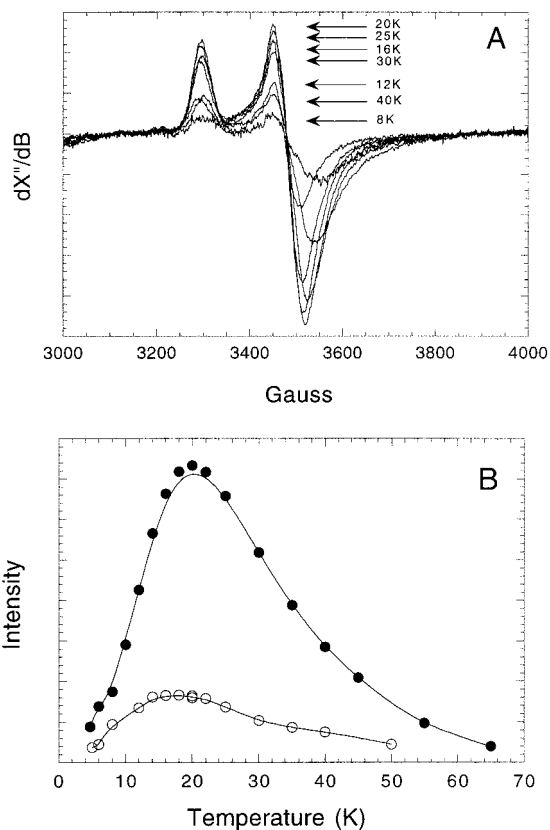


FIGURE 4: Temperature dependence of the EPR intensity for BioB reduced with dithionite in aqueous buffer. (A) EPR spectra of BioB following 90 min reduction with dithionite. (B) Temperature dependence of the $g = 1.93$ resonance for the 10 and 90 min reduced samples. Both samples show a maximal signal intensity at 20 K, typical of $[4\text{Fe-4S}]^{1+}$ clusters. Spectra were recorded at 4–70 K with other EPR parameters as indicated in Materials and Methods.

was likely due to dissociation of iron from the protein. In the presence of dithionite, the majority of free iron would be expected to be Fe^{2+} , with no visible absorbance or EPR signal. We directly followed the formation of free iron, using 30 kDa centrifugal concentrators to separate free iron from protein-bound iron. The buffer that passed through the concentrator was analyzed for total iron (33) and shows a rise in the concentration of free iron immediately following reduction (Figure 2B). The free iron concentration reaches a maximum concentration of $\sim 80 \mu\text{M}$ at 20 min and then slowly decreases. Similar results were seen for WT BioB (dashed curve) and His_6 -BioB (solid curve). The concentration of free iron measured is significantly less than the total iron in the samples ($800 \mu\text{M}$), suggesting that the dissociated iron remains weakly bound to the protein. Indeed, when we reduce a sample for 10 min and then add EDTA (1 mM), we can rapidly strip all of the iron from the protein and detect this iron in the buffer, suggesting that iron is bound much more weakly to the intermediate protein than to the initial $[2\text{Fe-2S}]^{2+}$ or final $[4\text{Fe-4S}]^{2+}$ proteins. The rates of release and reabsorption of iron by the protein in aqueous buffer are comparable to the rates of reduction and cluster formation observed by UV/visible spectroscopy for protein in 60% ethylene glycol.

Equilibration of $[2\text{Fe-2S}]^{2+}$ BioB with Excess Iron and Sulfide Results in Formation of Two $[4\text{Fe-4S}]^{2+}$ Clusters per Dimer. Conversion of the $[2\text{Fe-2S}]^{2+}$ clusters to $[4\text{Fe-4S}]^{2+}$ clusters in BioB apparently requires a strong reductant such

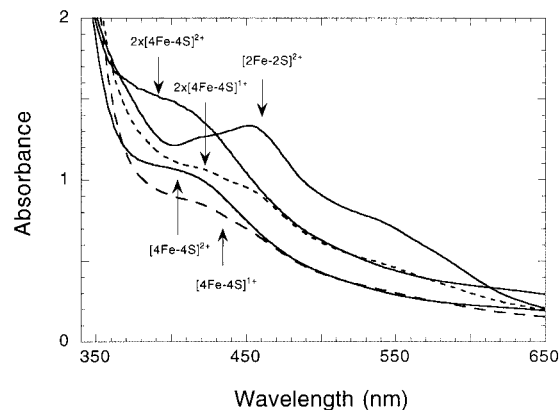


FIGURE 5: UV/visible spectra of various cluster forms in BioB. The initial $2 \times [2\text{Fe-2S}]^{2+}$ protein ($200 \mu\text{M}$), with a typical absorption band at 452 nm, is reductively converted to $[4\text{Fe-4S}]^{2+}$ protein in 60% ethylene glycol, with a shoulder at 410 nm, or $[4\text{Fe-4S}]^{1+}$ protein in aqueous buffer (both $200 \mu\text{M}$ protein, $\sim 120 \mu\text{M}$ cluster). Incubation of BioB with Fe^{2+} , S^{2-} , and DTT results in formation of $2 \times [4\text{Fe-4S}]^{2+}$ protein, with an increased absorption band at 410 nm and significant absorption from 450 to 800 nm. Reduction of this protein with dithionite results in formation of a $2 \times [4\text{Fe-4S}]^{1+}$ protein, a green-gray protein with significant absorption across the entire UV/visible spectrum. The latter two spectra are samples that have been desalted to remove excess iron and sulfide; while this process results in ca. 2-fold dilution, precise protein concentrations are not known and extinction coefficients have not been determined.

as dithionite to reduce the $[2\text{Fe-2S}]^{2+}$ clusters and dissociate iron from the protein. This cluster conversion is not effected by either dithiothreitol or flavodoxin, FNR, and NADPH (data not shown), but these are the only reductants typically available in routine biotin synthase assays. Therefore it seems that reductive cluster conversion cannot be occurring during *in vitro* assays. Furthermore, exogenous iron is required for biotin synthase activity (17), and it seemed plausible that $[4\text{Fe-4S}]^{2+}$ clusters could be built up by addition of iron and sulfide to the existing $[2\text{Fe-2S}]^{2+}$ clusters without the requirement for reduction or dissociation of iron. Indeed, when we incubate $[2\text{Fe-2S}]^{2+}$ BioB in 60% ethylene glycol with dithiothreitol and 4 equiv of FeCl_3 and then titrate in sulfide, we find that the absorbance spectrum of the protein is dramatically altered (Figure 5), with a UV–visible spectrum that shows an absorbance centered at 410 nm, but that does not match the spectrum obtained in the absence of excess iron and sulfide, with increased absorbance over the range of 450–700 nm. Desalting under anaerobic conditions does not alter the UV/visible spectrum, indicating that only tightly bound clusters, and not free iron, contribute to this spectrum. The EPR spectrum of this sample is devoid of features, indicating the absence of EPR active clusters. We believe that this sample contains two diamagnetic $[4\text{Fe-4S}]^{2+}$ clusters per BioB dimer; this interpretation is consistent with EPR results described below.

Reduction of $2 \times [4\text{Fe-4S}]^{2+}$ Protein Results in Rapid Formation of $2 \times [4\text{Fe-4S}]^{1+}$ Protein. The protein obtained by direct reconstitution of $[2\text{Fe-2S}]^{2+}$ BioB apparently contains two $[4\text{Fe-4S}]^{2+}$ clusters per BioB dimer, as indicated by the UV/visible spectrum (Figure 5). This protein sample can be repurified by gel-filtration chromatography under anaerobic conditions and retains the original (diluted) optical spectrum, indicating no loss of bound iron or iron–sulfur clusters. Addition of dithionite to BioB containing two $[4\text{Fe-4S}]^{2+}$ clusters results in rapid reduction of the protein within

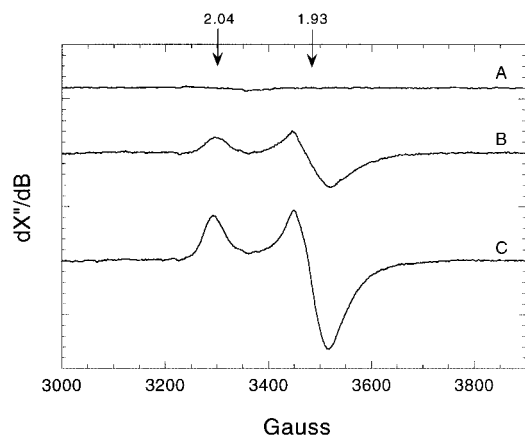


FIGURE 6: EPR spectra of various cluster forms of BioB (all samples are 200 μM). (A) The initial $[2\text{Fe-2S}]^{2+}$ sample contains no observable spin. (B) Reduction with dithionite in aqueous buffer results in formation of protein containing ~ 0.6 $[4\text{Fe-4S}]^{1+}$ cluster per BioB dimer. (C) Reduction of BioB reconstituted with Fe^{2+} , S^{2-} , and DTT results in formation of ~ 1.9 $[4\text{Fe-4S}]^{1+}$ clusters per BioB dimer. Both spectra exhibit g values of 2.04 and 1.93 and maximal signal intensity at $T = 20$ K, consistent with the presence of only $[4\text{Fe-4S}]^{1+}$ clusters.

the time required to mix the contents of the cuvette. The fully reduced protein has a broad, featureless UV/visible absorbance over the range from 350 to 600 nm (Figure 5) and a weak absorbance at ~ 800 – 900 nm (not shown); this spectrum is not the same as a scaled spectrum of BioB containing one $[4\text{Fe-4S}]^{1+}$ cluster per dimer. Following anaerobic desalting to remove free iron, the bound iron in the reconstituted and fully reduced protein was determined to be ca. 10 ± 2 Fe per BioB dimer, while the sample reduced in the absence of excess iron contains 2.4 ± 0.5 Fe per dimer. The slightly high iron content of reconstituted and reduced protein may reflect some adventitiously bound iron, while the low iron content of the directly reduced protein indicates the presence of residual apoprotein. The EPR spectrum of the fully reduced reconstituted protein is compared to the spectrum of a sample obtained by direct reduction of BioB with dithionite in the absence of excess iron in Figure 6. Spin quantitation indicates that the reconstituted and reduced protein contains ~ 1.9 $[4\text{Fe-4S}]^{1+}$ clusters per BioB dimer, while the sample reduced in the absence of excess iron contains ~ 0.6 $[4\text{Fe-4S}]^{1+}$ cluster per dimer. The temperature dependence of the EPR intensity indicates that all EPR-observable clusters are present as $[4\text{Fe-4S}]^{1+}$ clusters. The axial EPR spectrum with g values of 2.04 and 1.93 is typical of $[4\text{Fe-4S}]^{1+}$ clusters and is similar to spectra obtained for anRR (27), but these g values are slightly higher those found for other AdoMet-dependent radical enzymes (26, 28, 29). For example, the EPR spectrum of PFL AE with $[4\text{Fe-4S}]^{1+}$ clusters (in the presence of AdoMet) shows g values of 2.01 and 1.89 (26).

Rapid and Reversible Reduction and Oxidation of BioB Containing Two $[4\text{Fe-4S}]$ Clusters. We can now prepare samples of BioB that contain either two $[4\text{Fe-4S}]^{2+}$ or two $[4\text{Fe-4S}]^{1+}$ clusters per dimer; under anaerobic conditions these enzyme forms are completely stable. Previous experiments described above had indicated that the interconversion of these two enzyme oxidation states is particularly rapid. We followed the reduction of $2 \times [4\text{Fe-4S}]^{2+}$ BioB with dithionite in an anaerobic stopped-flow spectrophotometer

at 410 nm. The reduction is largely biphasic, with ca. 50% of the clusters reduced rapidly ($k_{\text{obs}} = 0.4 \text{ s}^{-1}$) and the remaining 50% over 10–20 s ($k_{\text{obs}} = 0.05 \text{ s}^{-1}$). We also followed the oxidation of $2 \times [4\text{Fe-4S}]^{1+}$ clusters with potassium ferricyanide at 410 and 452 nm. The oxidation occurred largely in a single phase, with 90% of the protein oxidized rapidly ($k_{\text{obs}} = 0.2 \text{ s}^{-1}$) and the remaining 10% oxidized much slower ($k_{\text{obs}} = 0.001 \text{ s}^{-1}$). UV/visible spectra of oxidized and reduced samples indicated that, over short time intervals (< 5 min), clean interconversion of 2+ and 1+ clusters occurred without net destruction of clusters. Oxidation with excess ferricyanide eventually results in destruction of the $[4\text{Fe-4S}]^{2+}$ clusters over 10–20 min. The observation of biphasic kinetics for reduction suggests that the two $[4\text{Fe-4S}]^{2+}$ clusters in BioB may differ either in accessibility to exogenous reductants or in equilibrium midpoint potential.

DISCUSSION

Conversions of $[2\text{Fe-2S}]$ and $[3\text{Fe-4S}]$ clusters to $[4\text{Fe-4S}]$ clusters have now been reported for all of the known AdoMet-dependent radical enzymes, including PFL AE (26, 35), lysine 2,3-aminomutase (28, 38), anRR (27), BioB (31), and LipA (29, 30). Although these enzymes differ in their ultimate mechanisms of catalysis, they are believed to share a common mechanism for activation of the enzyme via reductive cleavage of AdoMet and generation of a protein or substrate radical. Although little is known about the chemical details of this reaction, one plausible hypothesis is that flavodoxin-catalyzed reduction of the $[4\text{Fe-4S}]^{2+}$ cluster to a $[4\text{Fe-4S}]^{1+}$ cluster is followed by reductive cleavage of the AdoMet sulfonium. The resulting transient 5'-deoxyadenosyl radical abstracts a hydrogen from either the protein backbone or from substrate, generating a glyceryl or substrate radical. Consistent with this scenario, the chemically prepared $[4\text{Fe-4S}]^{1+}$ /AdoMet form of lysine 2,3-aminomutase is active in the absence of exogenous reductants (28).

An essential prerequisite in understanding the mechanism of the reaction involving AdoMet and the iron–sulfur cluster is an accurate understanding of the *in vivo* forms of enzyme. Anaerobic purification represents the most reliable method for accessing the *in vivo* clusters; for example, anaerobic purification of PFL AE allows the observation of a $[3\text{Fe-4S}]$ cluster (26), while exposure to even trace amounts of oxygen results in a mixture of several cluster types (35). Several attempts at anaerobic overexpression of BioB have resulted predominantly in the formation of inclusion bodies (J. Jarrett, unpublished results). Aerobic purification of BioB results in the high-yield isolation of the dimeric $[2\text{Fe-2S}]^{2+}$ protein. Initial reports by Flint and co-workers (5) suggested that dithionite reduction of the protein in aqueous buffer resulted in destruction of the cluster, although these observations were based upon UV/visible spectroscopy which does not easily detect reduced clusters. Johnson and co-workers (31) later reported that, in 60% ethylene glycol or glycerol, prolonged dithionite reduction resulted in slow formation of a $[4\text{Fe-4S}]^{2+}$ cluster. They suggest that reduction may result in the merger of two $[2\text{Fe-2S}]^{2+}$ clusters located at the dimer interface to form a single bridging $[4\text{Fe-4S}]^{2+}$ cluster and that cluster interconversion could represent a regulatory response to oxygen, allowing inactivation of the enzyme by reoxidation to $[2\text{Fe-2S}]^{2+}$ clusters in the presence of oxygen (31). In this model, the active enzyme is postulated to be

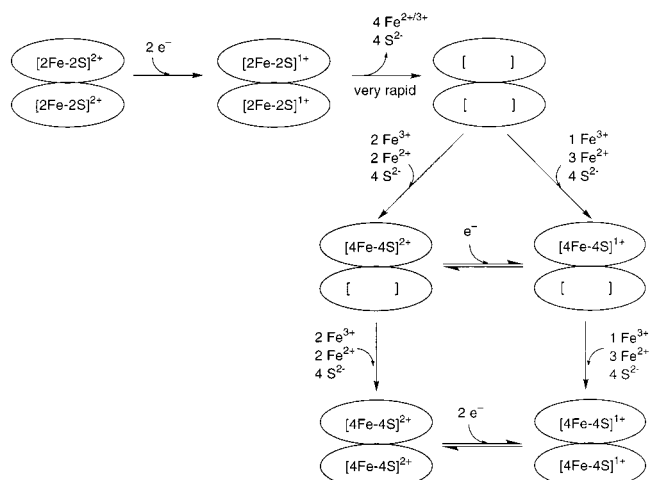
the BioB dimer containing one merged $[4\text{Fe-4S}]^{2+}$ cluster at the dimer interface.

We have demonstrated that formation of a $[4\text{Fe-4S}]^{2+}$ cluster in BioB does not occur through a “merging” of bound $[2\text{Fe-2S}]$ clusters but rather involves the dissociation and reassociation of iron from the protein. Following addition of dithionite in 60% ethylene glycol, we are able to observe the formation and decay of an intermediate that has little visible absorption and whose EPR spectrum shows primarily the broad high-field signal characteristic of free iron. We are able to chemically detect a corresponding increase in free iron, and we believe that this intermediate is likely to be predominantly apoprotein and dissociated iron. Consistent with this interpretation, the rate of the initial formation of this intermediate is not affected by iron chelators, while the subsequent formation of $[4\text{Fe-4S}]^{2+}$ protein is completely blocked by EDTA or histidine. Further, the formation of $[4\text{Fe-4S}]^{2+}$ enzyme is accelerated by the presence of excess iron, consistent with a second-order kinetic process involving free iron. However, the experiments described within this paper cannot rule out the possible presence of mononuclear Fe^{2+} bound either within the conserved cluster binding site or at other sites on the surface of the protein intermediate.

The role of ethylene glycol or glycerol in these reactions is unclear and is certainly not physiological. Reduction in the absence of ethylene glycol results in the rapid release of iron from the protein and the apparent formation of apoprotein, consistent with early observations of Flint and co-workers (5). However, reassociation of iron with the protein occurs over 15–60 min and one observes conversion to protein containing $\sim 0.6 [4\text{Fe-4S}]^{1+}$ cluster per dimer. Thus, we believe that ethylene glycol plays two roles in the previous experiments: first, it is clearly slowing the rate of iron association, allowing observation of an apoprotein intermediate, and second, it may be lowering the thermodynamic midpoint potential for the $[4\text{Fe-4S}]^{2+}/[4\text{Fe-4S}]^{1+}$ couple, resulting in formation of predominantly $[4\text{Fe-4S}]^{2+}$ protein. In other AdoMet-dependent radical enzymes it has been reported that the $[4\text{Fe-4S}]^{1+}$ redox state is inaccessible in the absence of AdoMet (26–30). It is clear that in the absence of ethylene glycol and glycerol, the $[4\text{Fe-4S}]^{1+}$ state is easily accessible in the BioB dimer in the absence of AdoMet, and this may allow an accurate determination of the midpoint potential.

The BioB dimer contains two conserved iron–sulfur cluster binding motifs, which in the aerobic protein contain two $[2\text{Fe-2S}]^{2+}$ clusters, and in the absence of added iron, the reassociation of iron and sulfide could result either in the formation of a bridging cluster (31) or in the formation of a $[4\text{Fe-4S}]^{2+}$ cluster in one monomer and an empty cluster binding site in the other monomer. We are not able to distinguish these possibilities with the present experiments. However, incubation of the enzyme with iron, sulfide, and dithiothreitol results in the direct formation of BioB containing two $[4\text{Fe-4S}]^{2+}$ clusters per dimer, and whose spectrum differs from the $[4\text{Fe-4S}]^{2+}$ enzyme produced in the absence of excess iron. BioB containing two $[4\text{Fe-4S}]^{2+}$ clusters per dimer is rapidly and completely reduced by dithionite with observed rate constants of 0.4 and 0.05 s^{-1} . The reduced protein has an EPR spectrum that is consistent with two $[4\text{Fe-4S}]^{1+}$ clusters per BioB dimer. Together, these results are consistent with the reactions summarized in Scheme 2, in

Scheme 2: Dithionite Reduction of BioB Dimer Containing Two $[2\text{Fe-2S}]^{2+}$ Clusters^a



^a The immediate product of reduction is presumably the $[2\text{Fe-2S}]^{1+}$ cluster, which is not observed due to the rapid dissociation of iron from the protein. In the absence of added iron, slow reassociation of iron and sulfide results in formation of BioB dimer that contains one $[4\text{Fe-4S}]^{2+}$ cluster per BioB dimer. In aqueous buffer, rapid reduction of this cluster results in formation of one $[4\text{Fe-4S}]^{1+}$ cluster per BioB dimer. In the presence of excess iron and sulfide, formation of two $[4\text{Fe-4S}]^{2+}$ clusters occurs in the presence of dithiothreitol. Reduction with dithionite results in rapid reduction to two $[4\text{Fe-4S}]^{1+}$ clusters per BioB dimer.

which formation of either one or two $[4\text{Fe-4S}]$ clusters per dimer is possible depending on the availability of excess iron.

A high-turnover assay for biotin synthase activity is currently not available, probably due to uncertainty regarding the *in vivo* sulfur donor (17, 39, 40), and therefore it is impossible to unambiguously identify the active form of the iron–sulfur cluster in biotin synthase. Rapid and facile interconversion of $[4\text{Fe-4S}]^{2+}$ and $[4\text{Fe-4S}]^{1+}$ clusters suggests that these may represent the native cluster forms in the active enzyme, but it is unclear whether the BioB dimer needs one or two clusters to catalyze AdoMet-dependent radical generation. Exogenous iron is required for activity *in vitro*, and therefore it seems plausible that maximal activity occurs when two $[4\text{Fe-4S}]$ clusters are present per BioB dimer. Our current model, that we hope to test with future experiments, is that the respective monomers of the BioB dimer are independently active for formation of one C–S bond in biotin. Thus BioB dimer that contains only one $[4\text{Fe-4S}]$ cluster would be active for formation of one C–S bond and would then release a 9-mercaptodethiobiotin intermediate (or a related compound) into solution. *In vitro* assays demonstrate that 9-mercaptodethiobiotin is chemically competent for conversion to biotin with retention of labeled sulfur (41). Binding of this intermediate by another half-active BioB dimer would catalyze complete thioether ring formation. One the other hand, BioB dimer that contains two $[4\text{Fe-4S}]$ clusters would be active for formation of both C–S bonds and would therefore release little or none of the proposed intermediate into solution. Differentiating these mechanisms will require a substrate-defined high-turnover assay that can be sustained in the absence of exogenous iron or reductants.

ACKNOWLEDGMENT

We thank Professor P. L. Dutton (University of Pennsylvania) for the generous use of his EPR spectrometer. We

also thank Professor J. B. Broderick (Michigan State University) for sharing results prior to publication.

REFERENCES

1. Cleary, P. P., and Campbell, A. (1972) *J. Bacteriol.* **112**, 830–839.
2. Rolfe, B., and Eisenberg, M. A. (1968) *J. Bacteriol.* **96**, 515–524.
3. Birch, O. M., Fuhrmann, M., and Shaw, N. M. (1995) *J. Biol. Chem.* **270**, 19158–65.
4. Ifuku, O., Kishimoto, J., Haze, S., Yanagi, M., and Fukushima, S. (1992) *Biosci. Biotechnol. Biochem.* **56**, 1780–5.
5. Sanyal, I., Cohen, G., and Flint, D. H. (1994) *Biochemistry* **33**, 3625–31.
6. Rodel, W., Plaga, W., Frank, R., and Knappe, J. (1988) *Eur. J. Biochem.* **177**, 153–8.
7. Sun, X., Eliasson, R., Pontis, E., Andersson, J., Buist, G., Sjoberg, B. M., and Reichard, P. (1995) *J. Biol. Chem.* **270**, 2443–6.
8. Ruzicka, F. J., and Frey, P. A. (1999) GenBank Accession No. AF159146.
9. Hayden, M. A., Huang, I., Bussiere, D. E., and Ashley, G. W. (1992) *J. Biol. Chem.* **267**, 9512–5.
10. Bianchi, V., Eliasson, R., Fontecave, M., Mulliez, E., Hoover, D. M., Matthews, R. G., and Reichard, P. (1993) *Biochem. Biophys. Res. Commun.* **197**, 792–7.
11. Harder, J., Eliasson, R., Pontis, E., Ballinger, M. D., and Reichard, P. (1992) *J. Biol. Chem.* **267**, 25548–52.
12. Blaschkowski, H. P., Neuer, G., Ludwig-Festl, M., and Knappe, J. (1982) *Eur. J. Biochem.* **123**, 563–9.
13. Knappe, J., Neugebauer, F. A., Blaschkowski, H. P., and Ganzler, M. (1984) *Proc. Natl. Acad. Sci. U.S.A.* **81**, 1332–5.
14. Moss, M., and Frey, P. A. (1987) *J. Biol. Chem.* **262**, 14859–62.
15. Ballinger, M. D., Frey, P. A., and Reed, G. H. (1992) *Biochemistry* **31**, 10782–9.
16. Ifuku, O., Koga, N., Haze, S., Kishimoto, J., and Wachi, Y. (1994) *Eur. J. Biochem.* **224**, 173–8.
17. Sanyal, I., Gibson, K. J., and Flint, D. H. (1996) *Arch. Biochem. Biophys.* **326**, 48–56.
18. Ohshiro, T., Yamamoto, M., Bui, B. T., Florentin, D., Marquet, A., and Izumi, Y. (1995) *Biosci. Biotechnol. Biochem.* **59**, 943–4.
19. Stubbe, J., and van der Donk, W. A. (1998) *Chem. Rev.* **98**, 705–62.
20. Frey, P. A. (1993) *FASEB J.* **7**, 662–70.
21. Magnusson, O. T., Reed, G. H., and Frey, P. A. (1999) *J. Am. Chem. Soc.* **121**, 9764–9765.
22. Mulliez, E., Fontecave, M., Gaillard, J., and Reichard, P. (1993) *J. Biol. Chem.* **268**, 2296–9.
23. Sun, X., Ollagnier, S., Schmidt, P. P., Atta, M., Mulliez, E., Lepape, L., Eliasson, R., Graslund, A., Fontecave, M., Reichard, P., and Sjoberg, B. M. (1996) *J. Biol. Chem.* **271**, 6827–31.
24. Wagner, A. F., Frey, M., Neugebauer, F. A., Schafer, W., and Knappe, J. (1992) *Proc. Natl. Acad. Sci. U.S.A.* **89**, 996–1000.
25. Moss, M. L., and Frey, P. A. (1990) *J. Biol. Chem.* **265**, 18112–5.
26. Broderick, J. B. (1999) Personal communication.
27. Ollagnier, S., Meier, C., Mulliez, E., Gaillard, J., Schuenemann, V., Trautwein, A., Mattioli, T., Lutz, M., and Fontecave, M. (1999) *J. Am. Chem. Soc.* **121**, 6344–6350.
28. Lieder, K. W., Booker, S., Ruzicka, F. J., Beinert, H., Reed, G. H., and Frey, P. A. (1998) *Biochemistry* **37**, 2578–85.
29. Busby, R. W., Schelvis, J. P. M., Yu, D. S., Babcock, G. T., and Marletta, M. A. (1999) *J. Am. Chem. Soc.* **121**, 4706–4707.
30. Ollagnier-de Choudens, S., and Fontecave, M. (1999) *FEBS Lett.* **453**, 25–8.
31. Duin, E. C., Lafferty, M. E., Crouse, B. R., Allen, R. M., Sanyal, I., Flint, D. H., and Johnson, M. K. (1997) *Biochemistry* **36**, 11811–20.
32. Bradford, M. (1976) *Anal. Biochem.* **72**, 248–254.
33. Beinert, H. (1978) *Methods Enzymol.* **54**, 435–45.
34. Berlyn, M. K. B., Low, K. B., and Rudd, K. E. (1996) in *Escherichia coli and Salmonella: Cellular and Molecular Biology* (Neidhardt, F., Ed.) pp 1715–1902, American Society for Microbiology Press, Washington, DC.
35. Broderick, J. B., Duderstadt, R. E., Fernandez, D. C., Wojtuszewski, K., Henshaw, T. F., and Johnson, M. K. (1997) *J. Am. Chem. Soc.* **119**, 7396–7397.
36. Kulzer, R., Pils, T., Kappl, R., Huttermann, J., and Knappe, J. (1998) *J. Biol. Chem.* **273**, 4897–903.
37. Orme-Johnson, W. H., and Orme-Johnson, N. R. (1982) in *Iron-Sulfur Proteins* (Spiro, T. G., Ed.) pp 67–96, John Wiley and Sons, New York.
38. Petrovich, R. M., Ruzicka, F. J., Reed, G. H., and Frey, P. A. (1992) *Biochemistry* **31**, 10774–81.
39. Bui, B. T., Florentin, D., Fournier, F., Ploux, O., Mejean, A., and Marquet, A. (1998) *FEBS Lett.* **440**, 226–30.
40. Gibson, K. J., Pelletier, D. A., and Turner, I. M., Sr. (1999) *Biochem. Biophys. Res. Commun.* **254**, 632–5.
41. Marquet, A., Frappier, F., Guillerme, G., Azoulay, M., Florentin, D., and Tabet, J.-C. (1993) *J. Am. Chem. Soc.* **115**, 2139–2145.

BI9926227